J Nanostruct 9(3): 453-467, Summer 2019

RESEARCH PAPER

Improved Curing Conditions and Mechanical/Chemical Properties of Nitrile Butadiene Rubber Composites Reinforced with Carbon Based Nanofillers

Mehran Sadeghalvaad [1,5,], Erfan Dabiri [2,5], Sara Zahmatkesh[3], Pooneh Afsharimoghadam [4]*

[1] *Nano Chemical Engineering Department, Faculty of Advanced Technologies, Shiraz University, Shiraz, Iran*

[2] *Department of Gas Engineering, Ahwaz Faculty of Petroleum, Petroleum University of Technology, Ahwaz, Iran*

[3] *Department of Materials Science and Engineering, Faculty of Engineering, Shiraz University, Shiraz, Iran*

[4] *Department of Earth Sciences, College of Science, Shiraz University, Shiraz, Iran*

[5] *Nano Chemical Engineering Department, Radin Faradid Petrosanat Co., Fars Science and Technology Park, Shiraz, Iran*

ARTICLE INFO

Article History:
Received 23 March 2019
Accepted 28 May 2019
Published 01 July 2019

Keywords:
Carbon Base Nanofiller
Carbon Nano Fiber
Mechanical Properties
Nanocomposite
Nitrile Rubber

ABSTRACT

Multiwall carbon nanotubes (MWCNTs) and carbon nanofibers (CNFs) with contents ranging from 1 to 10 phr (part per hundred parts of rubber) were selected and then characterized to reinforce acrylonitrile butadiene rubber (NBR) based composites. Fabrication of nanocomposites were done by a novel procedure and structural analysis along with variety of mechanical and chemical tests, according to the standard methods, were implemented to evaluate their properties. As a result, cure conditions, mechanical, and chemical properties of fabricated nanocomposites were further improved and optimized. The NBR nanocomposite containing 10 phr of MWCNTs devotes the best performance in curing time (13.3 % reduction), shore A hardness (36.4 % improvement), compression set (12.2 % reduction) and swelling rate in methyl ethyl ketone solvent (by the amount of 120 %) than those of other prepared nanocomposites and as a result, this nanocomposite was proposed as a material with the best improved properties for further industrial applications. However, 1 and 5 phr contents of MWCNTs were found to be optimum values of nanofillers to be added to the NBR in case of tensile strength and elongation at break properties.

How to cite this article
Sadeghalvaad M, Dabiri E, Zahmatkesh S, Afsharimoghadam P. Improved Curing Conditions and Mechanical/Chemical Properties of Nitrile Butadiene Rubber Composites Reinforced with Carbon Based Nanofillers. J Nanostruct, 2019; 9(3): 453-467.
DOI: 10.22052/JNS.2019.03.007

INTRODUCTION

Elastomers containing polymeric chains with high flexibility and mobility will show the same elasticity as that of the rubber, resist against large deformations and have high energy absorption properties, if polymeric chains are connected to the structure of network [1]. The world requires reduction in fuel consumption, and decrease of operating, production, and transportation costs. As a result, demands for novel materials with light weights, low costs, and high performances are increasing [2]. Nanocomposites are the new category of polymers with high mechanical and thermal properties and good performances. These materials can be used as an alternative for metals in the industry [3].

In recent decades, rubber industries have been revolutionized by using nanofillers. On the other hand, fillers having particles with at least a dimension of less than 100 nm and can

* *Corresponding Author Email: m.sadeghalvaad@gmail.com*

disperse separately in the base rubber, are the focus of researchers and companies to improve properties of rubbers [4]. Nano scale fillers have high surface to volume ratios with respect those with micron sizes and accordingly, can increase the contact surface between the rubber and fillers causing the improvement in properties of nanocomposites with the nanofiller contents even less than 1 wt. % [5,6]. The purpose of using fillers in polymers is to reinforce and improve physical, thermal, and mechanical properties, flame retardancy, conductivity, abrasion resistance, friction reduction, thermo-oxidative stability, ultraviolet waves and sound absorption [5,7,8]. Size and shape of nanofillers are important factors in polymeric composites reinforced with nanoparticles. In other words, high aspect ratio resulting from the formation of more free surface and interphase boundary between the polymer and filler can contribute to more affection due to the presence of nanofillers in polymer matrix. Carbon nanotubes (CNTs) and carbon nanofibers (CNFs) are from the category of those nanofillers with high aspect ratios [9].

Acrilonitrile butadiene is a commercialized and artificial rubber with applications not only in pieces of automobiles, but also in other industries like aerospace. In general, artificial rubbers do not have reinforcing properties alone because in their fabrication process, under strain crystallization will not be used in their preparation process (the same as what will be used for the natural rubber). Therefore, utilizing fillers is an effective method to improve the properties of rubber. Among all fillers, those with nano scale size have the best performance in this regards [10]. CNTs are very interesting and astounding materials and their shapes can be assumed as the rolling of a graphene plane in the form of a cylinder (single wall CNTs) or rolling of some graphene planes (multiwall CNTs) in the shape of co-axial cylinders with interlayer interval equal to that of graphite, diameter of 1-50 nm, and length of a few micrometers to millimeters or even centimeters [1,11]. CNTs have interesting mechanical properties, high flexibility, low density, and proper optical and magnetic properties [11,12]. Nanometric geometry and high aspect ratio of CNTs, along with their appropriate properties have made these materials as an advanced and effective candidates to be utilized as nanofillers in polymer synthesis [11]. Resulting nanocomposites from the polymer and CNTs have different applications in aerospace and automobile industries, electronically pieces, electrochemical sensors, and shape memory polymers [11,13]. CNT/NBR nanocomposite can be used as an alternative to NBR because of high affinity between acrylonitrile groups (ACN) and CNTs and having no significant poisoning effect by CNTs on vulcanization process [14].

Carbon nanofibers (CNFs) have diameter and length in ranges of 50-2000 nm and 50-100 µm, respectively. They have high modulus of elasticity and tensile strength along with proper electrical and thermal properties. Although modulus of elasticity of CNFs is much less than that of CNTs, they have the advantage of easier fabrication than that of CNTs [9]. Conventional methods for fabrication of elastomeric carbon based nanocomposites in the literature are melt mixing, solution blending, and in situ-polymerization [1]. Dispersing of rod shape nanoparticles in the polymer structure of composites are done by two methods of solution mixing and in-situ polymerization [12]. Among these two methods, in situ-polymerization is the most applicable one in this issue [15]. Dispersing of rod shape nanofillers in the polymer matrix have significant effect on the properties of nanocomposites in a way that well dispersing of them can contribute to improvement in the obtained properties [12,16]. Dispersing these anisotropic nanofillers in the polymer matrix can alter the properties of load transfer [7].

Holkkanen et al. showed that the preparation method of composite have direct impact on the dispersion of CNTs in the polymer matrix and accordingly, the resulting properties of the nanocomposite. Presence of carbon black nanoparticles in the nanocomposite can help the proper dispersion of rod shape nanofillers in the polymer matrix [17]. Limited researches have been done on the curing and vulcanization of nitrile rubber composites reinforced with nanofillers [8]. Perez and his coworkers probed into the curing characteristics of styrene and nitrile butadiene rubber nanocomposites endowed with CNT nanofillers by the method of Dynamic Scanning Calorimetry (DSC) [18].Wu and Chang investigated on carbon base fillers (carbon black, CNF, and CNT) and their affections on the epoxy curing features. They concluded that existence of these fillers in the polymer matrix can increase the heat of reaction, accelerate the curing reaction

(vulcanization) and cause the curing reaction to be done at lower temperatures with respect to the case in which these nanofillers are not used in the process of curing [19]. In the other work, mechanical and chemical properties along with the curing conditions of nanocomposites containing different nanofillers were evaluated and compared with each other [20].

The effect of adding nanofillers of single wall carbon nanotube and silica on the properties of natural rubber was investigated by Kueseng et al. They added nanofillers to a solution of natural rubber and then evaporated the solvent. Results of their prepared nanocomposites were concluded to be improved [21]. Fibrous structures have distinct properties which can be utilized for further industrial applications [22,23]. Mondal and his coworkers applied two methods of melt mixing and solution mixing to fabrication of CNF/chlorinated polyethylene. Solution mixing was found to be the better method than the other one in case of mechanical, electrical, and electromagnetical properties of prepared nanocomposites because of the fine distribution of CNFs in the composite by this method [24]. A quantitative analysis for dispersion degree of CNFs and CNTs in the polymeric nanocomposites were done by Luo et al. They concluded that the less nanoparticle size will result in the more challengable dispersion of nanofillers in the polymer matrix [25]. Tang and his research team probed into the dispersion effect of Graphene nanofillers on the mechanical properties of Graphene/Epoxy nanocomposite. They concluded that the more dispersion of the thermally reduced Graphene oxide nanoparticles will contribute to the more improvement in glass transition temperature (T_g), mechanical strength, and fracture toughness of nanocomposites because the toughness playes an important role on the nanofiller/polymer interfacial fracture [26]. In another work, mechanical, thermal, and rheological properties of Graphene/Poly propylene nanocomposite was investigated with the method of melt mixing by Achaby et al. Fine dispersion of Graphenes in the polymer matrix along with the improvement in mentioned properties of their fabricated nanocomposites by raising contents of nanofillers in the polymer matrix were the main results of their research [27].

In this contribution, nanofillers of multi wall carbon nanotube (MWCNT) and carbon nanofiber (CNF) were used to fabrication NBR based nanocomposites. Carbon black nanofiller was also applied to proper curing of nanocomposites and also fine dispersion of nanofillers in the polymer matrix. High resolution transmission electron microscope (HRTEM), and X-ray diffraction (XRD) analysis of nanofillers along with curing features, fourier transform infrared spectroscopy (FTIR) analysis, mechanical, and chemical properties of prepared nanocomposites (CNT/NBR and CNF/NBR) were evaluated and compared with each other to propose the best nanocomposite with optimum concentration in this regards.

MATERIALS AND METHODS

Constituent components for preparation of rubber composites including Polymer as the matrix, fillers, vulcanization agents, curing agents, reaction accelerators and anti-oxidation agents were purchased from the local market and are shown in Table 1.

Carbon black nanoparticles (with particle size of 70-96 nm) were used as the filler to improve the performance, dispersion and reduce fabrication costs of nanocomposites. According to the initial studies, carbon nanofiber (CNF) and multiwall carbon nanotube (MWCNTs) nanoparticles were selected to add to the polymer based composite. These nanoparticles were purchased from Sigma Aldrich Company, Germany and their properties are illustrated in Table 2.

Various techniques can be applied to stabilize nanofillers in the nanocomposite structure including functionalizing the surface of nanoparticle, utilizing ultrasonic waves (sonication), and centrifuging. Maximum amount of the based material (polymer) and concentration of used nanoparticles, as the filler are two principle factors in the stabilization process. Frequent methods for distribution uniformity analysis of nanoparticles in the aqueous solution are Scanning Electron Microscopy (SEM), Transmission Electron microscopy (TEM) and Atomic Force Microscope (AFM), while SEM and TEM analysis have priority for dispersion analysis of CNT and CNF nanoparticles [28–30].

Contents of additive materials for preparation and curing of nanocomposites are based on parts per one hundred rubber (phr) and amounts of these phr contents for used additives are the same for two studied nanocomposites. In this contribution, nanofillers of MWCNT and CNF with phr contents of 1, 3, 5, and 10 were selected to add

Table 1. Materials used to prepare nanocomposites.

Materials	Formula	Manufacturer
NBR 6240	Containing 34 % of Acrylonitrile	Local Market
Zinc Oxide	ZnO	Sigma-Aldrich
Carbon black (SRF)	----------	Local Market
IPPD Antioxidant (N-Isopropyl-N'-phenyl-p-phenylenediamine)	$C_{15}H_{18}N_2$	Local Market
Stearic acid	$CH_3(CH_2)_{16}COOH$	Sigma-Aldrich
RD Antioxidant (1,2-Dihydro-2,2,4-trimethylquinoline homopolymer)	$C_{12}H_{15}N$	Local Market
Hydrochloric Acid	HCl	Sigma-Aldrich
Plasticizer (Dioctyl phthalate)	C_6H_4-1,2-$[CO_2CH_2CH(C_2H_5)(CH_2)_3CH_3]_2$	Sigma-Aldrich
N-Cyclohexyl-2-benzothiazolesulfenamide	$C_{13}H_{16}N_2S_2$	Local Market
Accelerator (Tetramethylthiuram Disulfide)	$(CH_3)_2NCSS_2CSN(CH_3)_2$	Sigma-Aldrich
Octadecyl amine	$(CH_3(CH_2)_{16}CH_2NH_2)$	Sigma-Aldrich
Sulfur	S	Sigma-Aldrich
Distilled Water	H_2O	Local Market

Table 2. Properties of nanomaterials used for this paper (presented by their produced company).

Properties	Carbon nanofiber	Multiwall carbon Nanotube
Appearance	Black Powder	Powder
Impurities	Iron < 100 ppm Iron-free	----
Purity	> 95%	Carbon ≥ 98%
Average diameter (nm)	130	12
Pore size (Å)	124	----
Specific surface area (m^2/g)	24	220
Melting point (^0C)	3697-3652	3652-3697
Density (g/ml)	1.9	2.1
Dimension (O.D. × I.D. × L)	100 nm (D) × 20-200 µm (L)	6-13 nm × 2.5-20 µm

Table 3. Constituent components of fabricated nanofiller/NBR nanocomposites.

Materials	Mixing Condition (Phr)				
	NBR	1 Nano-NBR	3 Nano-NBR	5 Nano-NBR	10 Nano-NBR
NBR	100	100	100	100	100
Nanomaterials	0	1	3	5	10
Carbon Black (SRF)	80	80	80	80	80
ZnO	5	5	5	5	5
Stearic acid	1	1	1	1	1
RD	2	2	2	2	2
IPPD	1	1	1	1	1
DOP	10	10	10	10	10
Sulfur	0.5	0.5	0.5	0.5	0.5
TMTD	1	1	1	1	1
CZ	2	2	2	2	2

to the polymer matrix. Components mixing was done by the procedure in which nanomaterials were initially mixed by a two roll mill (Brabender, OHG model, Germany) at the mixing condition of the rubber (160 ^0C) and according to the standard method of ASTM D3187. Other components, including carbon black filler, DOP plasticizer, stearic acid, zinc oxide as an activator, anti-oxidizers of IPPD and RD were also added to the mixture of rubber and nanomaterials by the application of the two roll mill. Table 3 illustrates amounts of all additives for curing of the nanocomposites. For the purpose of investigating the effect of changing nanomaterials contents on the results of nanocomposites, a constant mixing time duration for the fabrication of all samples were

considered. Furthermore, the kind and amounts of nanomaterials were only variable parameters in the system. After one day and at the ambient temperature, materials which were considered for the process of nanocomposite curing, including the sulfur and accelerators, were added to the previous mixture by the two roll mill to prevent partial curing of the mixture. Distribution uniformity of nanoparticles in the polymer matrix is an outstanding factor regarding the properties of fabricated nanocomposites. For instance, distribution of nanoparticles in the NBR matrix have a profound impact on stress concentration spots and accordingly, an affection on the strength and failure properties of nanocomposites [31]. The same method was also applied for preparing the witness sample in which nanomaterials are not used.

A rheometer device (model of Gotech, Taiwan) was utilized for determining curing features of nanocomposites at the temperature of 160 ^{0}C and according to the standard method of ASTM D20148. Scorch time (ts_2) and optimum curing time (t_{90}) are two important parameters which were obtained from figures of rheometer device. Scorch time is the time duration in which the amount of torque is increased by 2.26 * 10^{-2} N.m with respect to the minimum amount of the torque. The less the amount of scorch time caused the cross-linking between mixing materials to be increased. Another outstanding parameter is optimum curing time which is the time when we reach to the rate of 90 % for the difference between the minimum and maximum amounts of the torque. This parameter can give us a proper evaluation on the amount of curing time for mixtures. The less the amount of optimum curing time, the faster fabrication of nanocomposites.

Nanoparticles were characterized by high resolution TEM, XRD, and FTIR analysis. Their related nanocomposites were also analyzed by the FTIR spectroscopy. A spectrometer (model of Perkin Elmer, USA) was used for the FTIR analysis. This technique is based on the absorption of radiation and probing into vibrational jumps of molecules and multi-atomic ions and standard of ISO 4650:2012 was used in this issue [32]. XRD pattern were obtained through X-ray powder diffraction (D8 Advance Bruker X-ray diffractometer with monochromatized Cu Kα=1.5418 Å). The crystallite size of samples were calculated by Williamson-Hall Approach [33]:

$$\beta \cos\theta = \frac{0.9\lambda}{d} + 2A\,\varepsilon \sin\theta \quad (1)$$

In this equation, d is the mean diameter of particles, λ is the wavelength of incident X-ray (equal to 1.5418 Å) , β represents the full width of the peak at half height (FWHM), ε is the lattice strain, and constant A is equal to 1.

Mechanical Properties

Shore Hardness

Hardness of a material is its strength against indentation by a harder material. In the standard hardness tests which have been used in recent years, a hard indenter material will be pressurized to the surface of the sample. As a result, a three directions tension will be imposed in the pressurized spot. On the other hand, transformation is done in combination with forms of tensile, compressive, and shear. Shore hardness test was done according to the standard method of ASTM D2240. For the test of rubbers, shore A hardness test is used. For determination of the shore A hardness test of nanocomposites, samples with thickness of at least 4 mm are placed on an aligned horizontal hard surface. Shore durometer type of A (code ISH-SAM) will then be rotated to the vertical position somehow that the indenter point has at least 9 mm distance from each edge of the sample. Base of the squeezer, in a way that its surface is parallel to that of the sample, is lifted quickly and without imposing strike. Degree of the indicator device is read after 15 seconds. This process was repeated for five different spots of the sample with intervals of minimum 6 mm from each other. Averages of obtained values are considered as the shore A hardness. Depth of indentation, D (mm), which is a criteria for evaluation of the hardness is determined by the following equation [34]:

$$D = 100 - \frac{h}{0.025} \quad (2)$$

Where h (mm) is the depth of indentation at the time of imposing the whole force. With this method, the amount of penetration for the indenter to the material is measured in specified conditions.

Tensile Strength

This test was conducted based on the standard method of ASTM D412 for dumbbell shaped test

piece. Length of the dumbbell shaped samples are 20±0.5 mm and the nominal speed of the moving clipper is also 500 mm/min according to the mentioned standard method. All used molds and blades were based on the standard of ISO 4661-1:1993 and molds were also in the standard dimension for preparation of dumbbells. In each point of the thin width mold, deviation from the state of parallel edges should not be larger than 0.05 ml. The device for doing the tensile test should also be in line with the standard condition of ISO 5893:1993. Thickness at the center and two end points of the test piece were measured by the thickness tester and the average measured amounts of surface area were used. In each dumbbell, none of three measured thin section values should have difference from the average thickness by the amount of more than 2%. Test piece was placed in the tensile test device in a way which lateral and parallel sections at two end points of the test piece were fixed symmetrically and pressure was distributed uniformly on the surface area. The device was turned on and with the nominal velocity of 500 mm/min for the moving pine, changes in amounts of length and force during experiments were measured with the accuracy of ±2 %. Tensile strength TS (MPa) was determined by:

$$TS = \frac{F_m}{Wt} \quad (3)$$

Where F_m (N) is the maximum amount of recorded force, W (mm) is width of the mold thin section, and t (mm) is the thickness of the test piece. Tensile strength at the breaking point (TS_b) was also obtained by this equation:

$$TS_b = \frac{F_b}{Wt} \quad (4)$$

Where F_b is the recorded force at breaking point.

Elongation at Break

The ability of large deformation of a material is calculated by the parameter of elongation at break. It indicates strength of the whole molecular chains and their movement [35]. Elongation at break (in percentage) of nanocomposites were obtained according to the standard of ASTM D412 and by the following equation [36]:

$$E_b = \frac{100*(L_b - L_0)}{L_0} \quad (5)$$

Where E_b is elongation at break, L_b (mm) is length of the test device at breaking point and L_0 (mm) is its initial length, respectively.

Compression Set

As the rubber is under pressure, physical and chemical changes can occur in its structure leading to prevention of the rubber to return to its initial dimension after release of the deformation force. Consequently, the amount of compression set for the rubber depends on the time and temperature of the compression and is also dependent on the time and returning temperature. Compression set (C) is determined in the percentage form of the initial compression as follows:

$$C = \frac{h_0 - h_1}{h_0 - h_2} \times 100 \quad (6)$$

Where h_0 is the initial thickness of the test piece, h_1 is its thickness after returning, and h_2 is the height of spacing. All dimensions are in the scale of millimeter. This test was done in accordance to the standard method of ASTM D395 [37].

Chemical Properties

Ozone Resistance

In this test, a relative estimation is done on the resistance of the rubber components against weathering in the open space and or in the ozone container (Based on the standard of ASTM D2240). For conducting this experiment, rubber piece was placed on the ozone container according to the information mentioned in the Table 4. After probing into the rubber piece, if no cracks or fractures was observed on the surface of the sample, the test sample is considered to be resistant against the ozone.

Fluid Resistance

To check the resistance of rubbers against liquids or chemical solutions, different solvents are used. According to the literature and different standards, Methyl Ethyl Ketone (MEK) solvent is

Table 4. Conditions of conducting test for resistance of the rubber against ozone [ASTM D2240]

Test Condition	Amount
Ozone Concentration (g/l)	$(50\pm5)\times10^{-8}$
Temperature (°C)	40±2
Time of Exposure to Ozone (hr)	48
Elongation (%)	20±2
Relative Humidity	55±5

a proper choice in this regards (It was purchased from Merck Millipur Company). Method of conducting this experiment is in this way that the sample was firstly weighed (W_1) and was then put into the solvent of methyl ethyl ketone at 30 ^{0}C. After 48 hours, swollen sample was extracted from the solvent and completely dried under the Vacuum Oven [model of Vin100, Arta Company, Iran] and was weighed again (w_2). The rate of swelling was then calculated from the following equation [38].

$$\%Swelling = \frac{w_2 - w_1}{w_1} \times 100 \quad (7)$$

RESULTS AND DISCUSSION

Features of Nanocomposites Curing

Table 5 shows rheometry data of fabricated composites and nanocomposites. In general, torque will increase by adding nanoparticles (MWCNT and CNF) and raising their contents in the NBR based matrix. Results indicate that using MWCNT nanoparticles in curing of nanocomposites will decrease the time duration for cross linking creation. This trend for the decrease of nanocomposite curing was also observed for nanocomposites containing 5 and 10 phr of CNFs. As a result, time duration for final curing of the product will be decreased by reduction of t_{90}.

Characterization

Imaging

Fibrous structure, nano scale size, and unique morphology of CNF were concluded from its HRTEM image, as is shown in Fig. 1 (A). This nanoparticle which is already an individual nanofiber, has a hollow core surrounding by a cylindrical fiber consisted of crystalline, graphite

Table 5. Rheometry data of studied nanocomposites.

		Torque (N.m)		Time (min)	
Sample		T_{min}	T_{max}	ts_2	t_{90}
NBR Composite		0.46	1.97	1.43	20.10
	Phr				
MWCNT/NBR Nanocomposites	1	0.48	2.08	1.41	20.00
	3	0.49	2.25	1.38	19.58
	5	0.50	2.35	1.20	18.10
	10	0.52	2.51	1.08	17.42
CNF/NBR Nanocomposite	1	0.49	2.20	1.42	20.03
	3	0.51	2.32	1.39	19.80
	5	0.53	2.45	1.27	19.60
	10	0.55	2.62	1.20	18.10

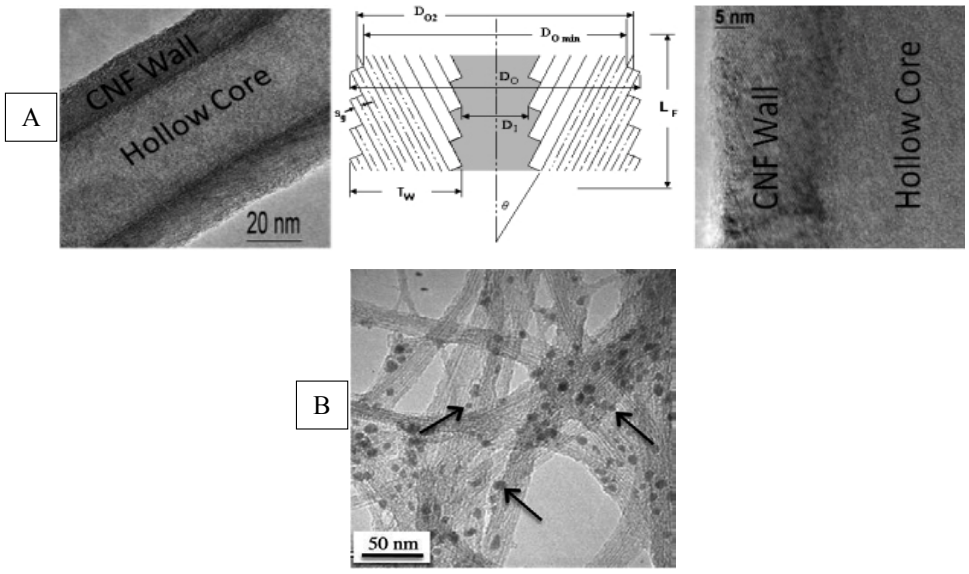

Fig. 1. HRTEM images of CNFs and MWCNTs (A and B, respectively).

basal stacked at 25 degrees from the longitudinal axis of the fiber. A fiber with exposed edge planes along the whole interior and exterior surfaces of the nanofiber is generated from this morphology. Mechanical reinforcement in polymer composite is attained from this generated fiber. CNFs have average diameters around 130 nm, while their length are in the range of 20-200 µm (HRTEM image of CNFs and the above description were from the information that the purchaser company (Sigma-Aldrich) provided us and also from references [39,40].

Fig. 1 (B) shows also HRTEM image of bundles of MWCNTs and arrows in the figure illustrate iron-based catalyst nanoparticles on the sidewalls of the nanoparticle [40]. Average diameter and length of MWCNTs were found to be around 12 nm and range of 2.5-20 µm, respectively, which are significantly lower than those of CNFs.

XRD Pattern

MWCNT and CNF nanofibers were characterized by XRD pattern, as are illustrated in Figs. 2 and 3, respectively. Fig. 2 shows clearly that two index peaks are existed in the structure of MWCNT [41]. These peaks are regarded to planes of '002' and '100', respectively [42]. Moreover, another peak is detected at 64.4111 diffraction angle related to the plane of '110'. Similarity between the represented peaks from XRD results of MWCNT and known index peaks of this structure confirms that purchased MWCNT nanoparticle has suitable structure for further composite synthesizing. To measure the crystallite size of MWCNT, Williamson-Hall approach was utilized by the XRD results. The crystallite size of MWCNT was measured to be 11.27 nm. In addition, the lattice strain was reported to be 0.1052.

The XRD spectrum of CNF clearly depicts its

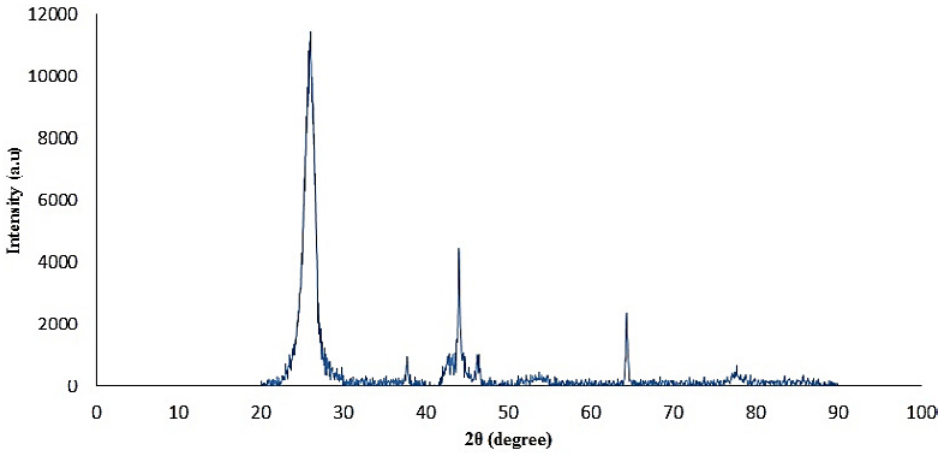

Fig. 2. XRD pattern for MWCNT nanoparticle.

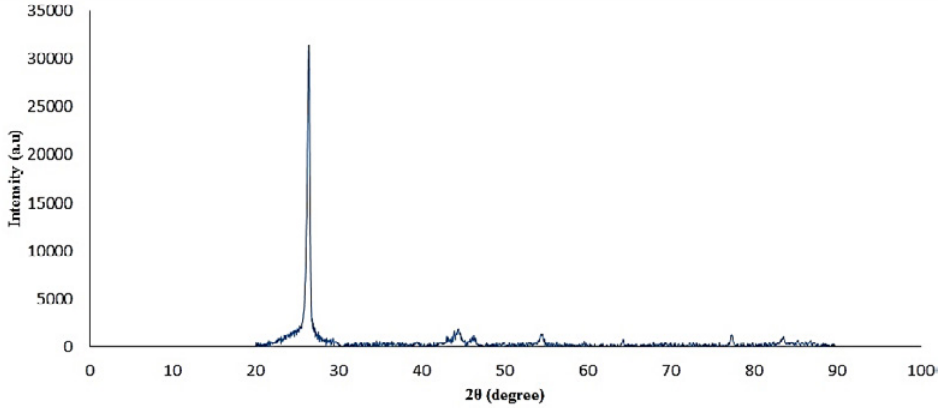

Fig. 3. XRD pattern for CNF nanoparticle.

three index peaks [43]. These peaks are obtained in 26.1990, 43.981, and 54.1852 diffraction angles related to the planes of '002', '100', and '101', respectively [44]. The mentioned peaks are totally corresponded to the known peaks of CNF. Similarly, the crystallite size of CNF was measured through Williamson-Hall equation using the XRD pattern. Crystallite size and lattice strain of purchased CNF were reported to be 2.27nm and 0.10425, respectively. Sharp XRD peak of CNF confirms this fact that crystallite size of CNF is very small because no obvious broadening is shown in its XRD pattern [45].

FTIR analysis

Figs. 4 (A and B) show the FTIR analysis of MWCNT nanoparticles and MWCNT/NBR nanocomposite, respectively. According to the Fig. 4 (A), two specific peaks for the studied MWCNT nanoparticles are at wave numbers of 1632 and 3440.44 cm^{-1} are related to the bond of C=C and tensile bond of –O-H, respectively [46]. After the preparation and curing of MWCNT/ NBR nanocomposite, these two peaks will slightly transit to reach wave numbers of 1632.93 and 3438.44 cm^{-1}, respectively, illustrating the presence of MWCNT nanoparticles in the structure

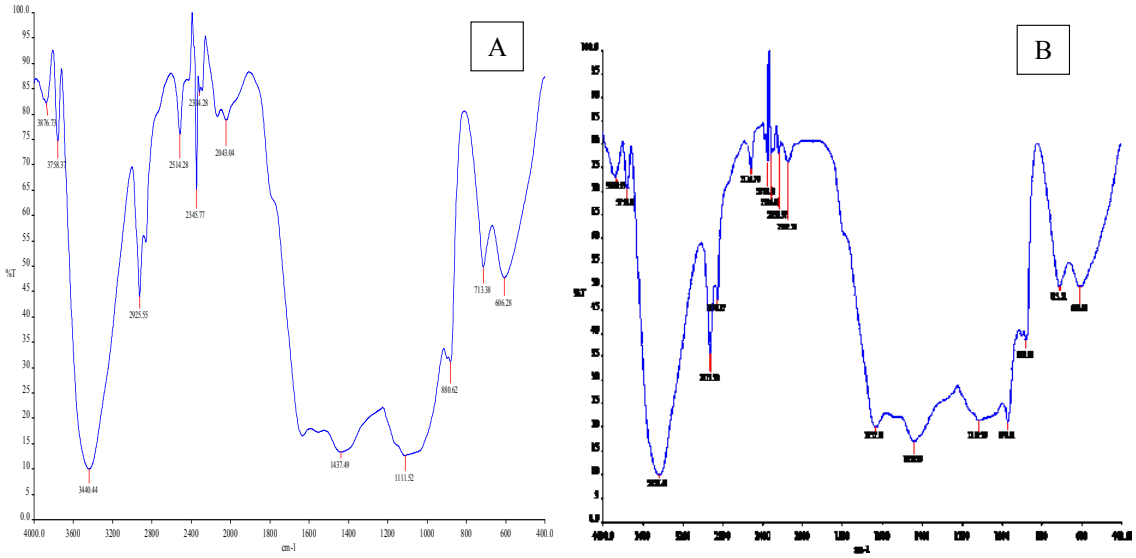

Fig. 4. FTIR analysis of MWCNT nanoparticles (A) and MWCNT/NBR nanocomposite (B)

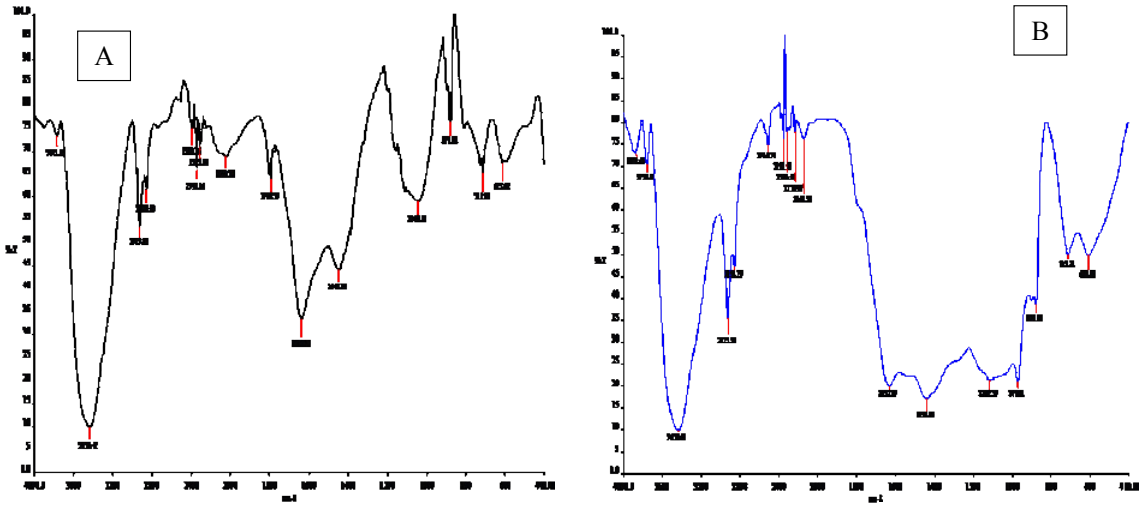

Fig. 5. FTIR analysis of CNF nanoparticles (A) and CNF/NBR nanocomposite (B)

of fabricated nanocomposite. Furthermore, other peaks at wave numbers of 970.81 cm^{-1} (for the bond of –CH=CH-), 1439.95 cm^{-1} (bond of –C=C-), 2336.97 cm^{-1} (bond of -C≡N), and 2925 cm^{-1} (for functional group of CH_2) are in the FTIR spectrum of MWCNT/NBR nanocomposite. As a consequence, simultaneous presence of peaks for two considered materials in the FTIR spectrum indicates the complete cure of MWCNT/NBR nanocomposite [46–48].

FTIR results of CNF nanoparticles and CNF/NBR nanocomposite are also illustrated in Figs. 5 (A and B), respectively. Observed peak at the wave number of 1636.80 cm^{-1} in the Fig. 5 (A) is related to the tensile bond of C=O in carboxylic acid group. At wave numbers of 2347.14 and 2923.98 cm^{-1}, resulted peaks are relevant to bond of O=C=O and tensile bond of C-H, respectively. In addition, the peak at 3439.42 cm^{-1} is also resulted from the hydroxyl functionalized groups on the CNF surface. Peaks at the wave number range of 2000 to 3000 cm^{-1} are related to the post treatment operations which were done after the preparation of CNF nanoparticles [49].

Investigation of the FTIR spectrum for CNF/NBR nanocomposite is shown in the Fig. 5 (B). Four peaks described for the CNF structure at wave numbers of 1632.93 cm^{-1} (tensile bond of C=O in the carboxylic acid group), 2350.59 cm^{-1} (double bonds of O=C=O), 2925.30 cm^{-1} (tensile bond of C-H), and 3438.44 cm^{-1} (hydroxyl functionalized group on the CNF surface) are all observed with a little transition because of the composite formation. Furthermore, the peaks at wave numbers of 970.81, 1439.95, 2336.97, and 2856.17 cm^{-1} are due the bonds of (–CH=CH–), (–C=C–), (-C≡N), and (CH_2); illustrating the presence of NBR in the CNF/NBR nanocomposite. It can be concluded that curing of composites were done in an appropriate way and after the curing, CNF/NBR nanocomposite was fabricated [47–49].

Mechanical Properties

Mechanical properties evaluation of fabricated nanocomposites were done and the results are shown in Fig. 6. Shore A hardness, tensile strength, elongation at break, and compression set of composites and nanocomposites were selected regarding their mechanical properties evaluation.

It is obvious in this figure that raising phr contents of nanofillers resulted in the increase of shore A hardness for their related nanocomposites. Adding nanofillers of MWCNF to the NBR matrix contributes to the more increase in shore A hardness of the resulting nanocomposite than that of CNF/NBR nanocomposite. The amount of shore A hardness for nanocomposites containing 10 phr

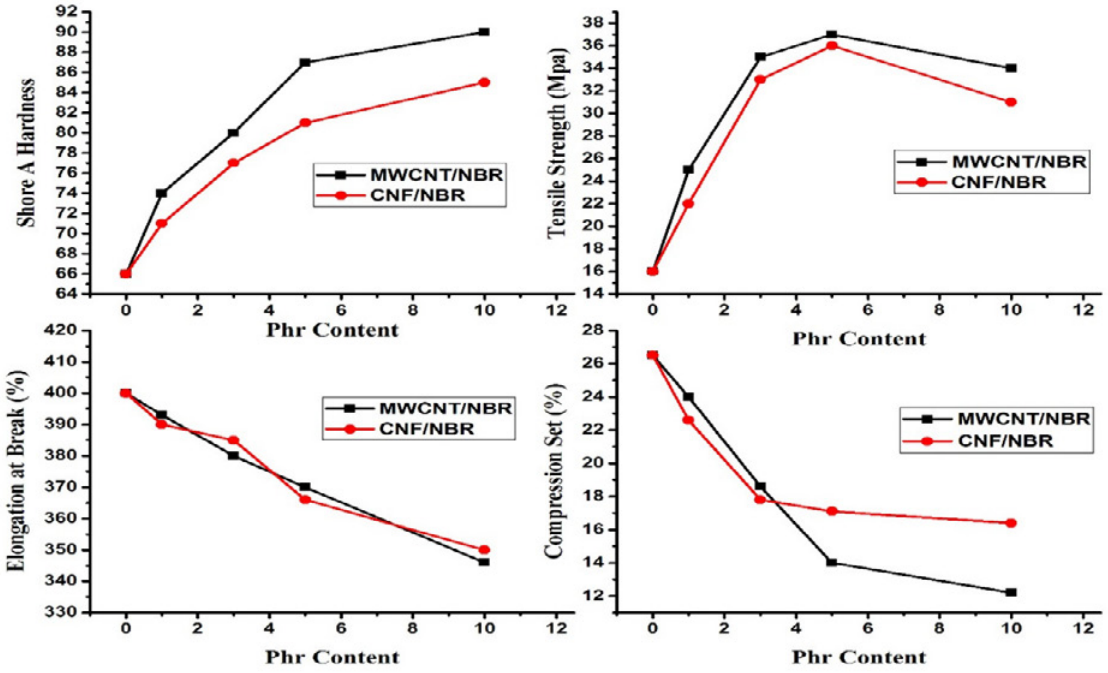

Fig. 6: Mechanical properties of fabricated nanocomposites versus Phr content.

of MWCNT and CNF are 90 and 85, respectively. The maximum percentage increase of this property for the nanocomposite with 10 phr of MWCNTs and CNFs are 36 % and 30 %, correspondingly, with respect to that of NBR.

Two important parameters which are used to determine tensile-stress-strain properties of nanocomposites are tensile strength and elongation at break. Generally, tensile strength of composites are directly dependent on their structure and behavior of their base matrix. If fillers are distributed properly in the matrix, tensile strength of the resulting composite will also be increased. However, for the case in which distribution of particles in the polymer matrix is asymmetric, tensile strength of the composite will be reduced because of the formation of concentrated tension points in the matrix. This behavior is obvious in fillers with micron sizes [31]. Nano scale structures in the same weight percentages as for the particles with micron sizes can tackle mentioned problem because of better distribution of nanoparticles in the matrix and also their smaller sizes. It should also be noted that less increase in weight percentages of materials in nano scale can improve different properties of the composite with respect to materials in micron scale [50,51]. It can also be detected from this figure that nanocomposite containing 5 phr of MWCNT nanoparticles has the maximum amount of tensile strength with respect to that of the other fabricated nanocomposite. In addition, MWCNT/NBR nanocomposite devoted the highest amount of tensile strength in the whole studied phr contents of nano additives with respect to that of CNF/NBR nanocomposite. Raising the amount of MWCNT and CNF nanoparticles to the amount of 5 phr caused the tensile strength of related nanocomposite to be increased, while the use of 10 phr of these nanoparticle in related nanocomposites leaded their tensile strength to be reduced in comparison to the use of 5 phr nanoparticle in NBR matrix. On the other hand, 5 phr of MWCNTs and CNFs are optimum values of nano additives to be applied to both nanocomposites in the case of improved tensile strength.

In addition, raising the amount of nanofillers in the nitrile rubber matrix decreased the elongation at break of fabricated nanocomposites. Elongation at break percentages for the NBR and MWCNT/NBR nanocomposite with 10 phr of its nano additive were 400 and 346, respectively, while percentage of elongation at break for CNF/NBR nanocomposite with 10 phr of nano additives were found to be 350. Elongation at break of nanocomposites with 1 and 3 phr contents of MWCNTs are higher than that of CNFs with the same phr contents. However, for the case in which 5 and 10 phr of nanomaterials were used in the NBR matrix, elongation at break percentages of CNFs showed to be more than that of MWCNTs.

Analysis of compression set test was done at 100 ^{0}C and for the time duration of 72 hours. Results indicate that adding nanofillers to the composites will reduce their deformation resulting from impose of the pressure force to structure of nanocomposites. High percentage values of compression set means constant deformation of rubber matrix in the compression form. A higher volume contents of nanofillers in the polymer matrix results in the higher dispersion and concentrations with respect to the volume and accordingly, decrease of the compression set [52]. Compression set for 5 and 10 phr of CNF/Nitrile rubber nanocomposites were slightly reduced. As a result, phr of 3 can be considered as the optimum amount of CNF nanoparticle in the related nanocomposite. For MWCNT/Nitrile rubber nanocomposite, compression set was reduced from 26.5% to 12.2 % by adding 10 phr of MWCNTs to the related composite. Comparing results for the compression set of studies nanocomposites indicate that adding 1 and 3 phr of nano additives to the composites caused MWCNT/NBR nanocomposite to have larger percentage of compression set than that of the other nanocomposite, while adding 5 and 10 phr of nano additives to CNF/NBR nanocomposite leaded its compression set percentages to have larger values with respect to those of the other one. Minimum value for the compression set percentage of the CNF/NBR was found to be 16.4 by applying 10 phr of the nanoparticle to the matrix.

Chemical Properties

Ozone Resistance

Results indicate that all prepared samples including pristine nitrile rubber and fabricated nanocomposites are resistant against the ozone because no crack was observed on the surface of samples during the time of conducting this test and at its specified condition.

Table 6. Swelling rate of prepared nanocomposites in MEK solvent.

Sample tests		Swelling in MEK Solvent (%)
Non-Vulcanized NBR		Will be solved
Vulcanized NBR		165
	Phr	
MWCNT/NBR Nanocomposites	1	160
	3	144
	5	124
	10	120
CNF/NBR Nanocomposite	1	163
	3	148
	5	134
	10	124

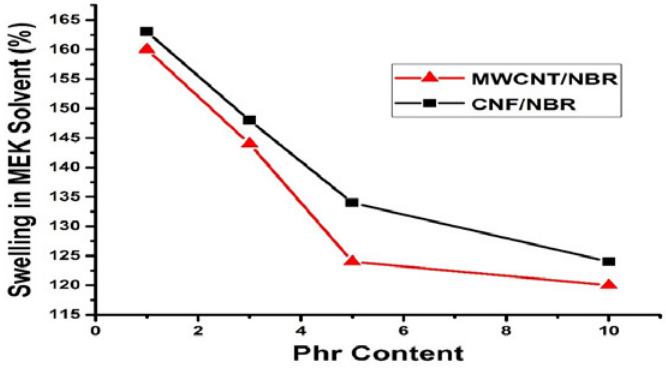

Fig. 7. Chemical Properties evaluation of fabricated nanocomposites versus Phr content

Resistance in Methyl Ethyl Ketone (MEK) Solvent

Table 6 shows the swelling rate of prepared nanocomposites in MEK solvent. Non-vulcanized NBR was completely solved in the MEK solvent, while vulcanized NBR did not solve in this solvent and their rate of swelling is dependent on their cross-linkings and nano additives. This table indicates that MWCNT/NBR nanocomposite has better barrier properties than the vulcanized NBR and CNF/NBR nanocomposite. With respect to the information available in literature [53,54] and Table 6, NBR nanocomposites containing MWCNT nanoparticles caused the swelling rate of final product to be reduced and accordingly, increased their resistance against the MEK solvent. However, this reduction in the swelling rate of the nanocomposite endowed with CNFs found to be less than that of MWCNT/NBR nanocomposite by further raising of the phr for nano additives in their structures. Comparative results of swelling rate for MWCNT/NBR and CNF/NBR nanocomposites can be observed in the Fig. 7.

CONCLUSIONS

Elastomeric nanocomposites consisting of MWCNTs and CNFs, as nanofillers in 5 different phr contents (0, 1, 3, 5, 10) and nitrile rubber were successfully fabricated and the interaction between nanoparticles and polymer matrix were analyzes by FTIR spectroscopy. Characterization of nanoparticles were also done for determining their suitability to mix with the nitrile rubber. According to the rheometry results and cure conditions, nanocomposite containing 10 phr of MWCNT nanofiller devotes the best curing conditions than the other fabricated nanocomposites indicating a reduction of 13.3 % in the curing time and increase of the fabrication rate for samples. Mechanical properties of composites and nanocomposites were analyzed and compared with each other. Obtained results for shore A hardness of nanocomposites with different phr contents indicates that the change of this property is increasing with raising of nanofiller contents. MWCNT/NBR nanocomposite with 10 phr of the nanofiller had the highest rate of shore A hardness among that of other ones by the increase percentage rate of 36.4 than that of the NBR. Investigation of tensile-stress-strain properties were done by considering two parameters of tensile strength and elongation at break for all prepared nanocomposites in different phr contents of nanofillers. The maximum value for tensile strength was attained for the NBR nanocomposite with 5

phr of MWCNTs with the amount of 37 Mpa and increase percentage rate of 131.3 than that of NBR. In addition, 1 phr MWCNT/NBR nanocomposite devotes the best performance for elongation at break percentage among other ones by the rate of 393 % and further raising the content of nanofiller contributes to the reduction of this property. At 10 phr contents of both nanocomposites, about 350 % of elongation at break was obtained indicating a reduction by the rate of 12.5 % for this property by the addition of nanofillers with 10 phr content to the polymer matrix with respect to that of NBR. The nanocomposite with 10 phr of MWCNTs were found to have the lowest and best value for compression set percentage (12.2%) than that of other fabricated nanocomposites. For evaluation of chemical properties for all composites and nanocomposites, resistance against ozone and methyl ethyl ketone (MEK) solvent of them were investigated. It was concluded that they are resistant against ozone and their swelling rates in MEK solvent were reduced by adding and raising the phr contents of nanofillers. The nanocomposite with 10 phr contents of MWCNT had the lowest swelling rate percentage in MEK solvent than that of other ones by the rate of 120 %. According to the improvement in considered properties and obtained results in this research, the NBR nanocomposite with 10 phr of MWCNTs is proposed as a material with optimized properties for further industrial application.

ACKNOWLEDGEMENT

Authors are grateful to the Fars Science & Technology Park for providing their equipped laboratories for them to successfully complete this work. I also acknowledge that the university we are affiliated with is fully aware of this submission, and the publication of the manuscript is approved by all authors and by the responsible authorities where the work was carried out. The interests of the coauthors of the manuscript do not conflict at all.

CONFLICTS OF INTEREST

The authors declare that there are no conflicts of interest regarding the publication of this manuscript.

REFERENCES

1. Bokobza L. Mechanical and Electrical Properties of Elastomer Nanocomposites Based on Different Carbon Nanomaterials. C. 2017;3(4):10.
2. Dabiri E, Bahrami F, Mohammadzadeh S. Experimental investigation on turbulent convection heat transfer of SiC/W and MgO/W nanofluids in a circular tube under constant heat flux boundary condition. J Therm Anal Calorim. 2017;131(3):2243-2259.
3. Garcés JM, Moll DJ, Bicerano J, Fibiger R, McLeod DG. Polymeric Nanocomposites for Automotive Applications. Adv Mater. 2000;12(23):1835-1839.
4. Galimberti M, Cipolletti V, Musto S, Cioppa S, Peli G, Mauro M, et al. RECENT ADVANCEMENTS IN RUBBER NANOCOMPOSITES. Rubber Chem Technol. 2014;87(3):417-442.
5. Schopp S, Thomann R, Ratzsch K-F, Kerling S, Altstädt V, Mülhaupt R. Functionalized Graphene and Carbon Materials as Components of Styrene-Butadiene Rubber Nanocomposites Prepared by Aqueous Dispersion Blending. Macromolecular Materials and Engineering. 2013;299(3):319-329.
6. Punetha VD, Rana S, Yoo HJ, Chaurasia A, McLeskey JT, Ramasamy MS, et al. Functionalization of carbon nanomaterials for advanced polymer nanocomposites: A comparison study between CNT and graphene. Prog Polym Sci. 2017;67:1-47.
7. Hajibaba A, Naderi G, Ghoreishy M, Bakhshandeh G, Nouri MR. Effect of single-walled carbon nanotubes on morphology and mechanical properties of NBR/PVC blends. Iranian Polymer Journal. 2012;21(8):505-511.
8. Likozar B. Modeling of chemical kinetics of elastomer/hydroxyl- and carboxyl-functionalized multiwalled carbon nanotubes nanocomposites' cross-linking. Polymer Engineering & Science. 2010;51(3):542-549.
9. Pingot M, Szadkowski B, Zaborski M. Effect of carbon nanofibers on mechanical and electrical behaviors of acrylonitrile-butadiene rubber composites. Polym Adv Technol. 2018;29(6):1661-1669.
10. Zhang Y, Park S-J. In-situ modification of nanodiamonds by mercapto-terminated silane agent for enhancing the mechanical interfacial properties of nitrile butadiene rubber nanocomposites. Polym Compos. 2017;39(10):3472-3481.
11. Pedroni LG, Soto-Oviedo MA, Rosolen JM, Felisberti MI, Nogueira AF. Conductivity and mechanical properties of composites based on MWCNTs and styrene-butadiene-styrene block™ copolymers. J Appl Polym Sci. 2009;112(6):3241-3248.
12. Fritzsche J, Lorenz H, Klüppel M. CNT Based Elastomer-Hybrid-Nanocomposites with Promising Mechanical and Electrical Properties. Macromolecular Materials and Engineering. 2009;294(9):551-560.
13. Le HH, Sriharish MN, Henning S, Klehm J, Menzel M, Frank W, et al. Dispersion and distribution of carbon nanotubes in ternary rubber blends. Composites Sci Technol. 2014;90:180-186.
14. Zhao Q, Tannenbaum R, Jacob KI. Carbon nanotubes as Raman sensors of vulcanization in natural rubber. Carbon. 2006;44(9):1740-1745.
15. Verge P, Peeterbroeck S, Bonnaud L, Dubois P. Investigation on the dispersion of carbon nanotubes in nitrile butadiene rubber: Role of polymer-to-filler grafting reaction. Composites Sci Technol. 2010;70(10):1453-1459.
16. Ponnamma D, Ramachandran R, Hussain S, Rajaraman R, Amarendra G, Varughese KT, et al. Free-volume correlation with mechanical and dielectric properties of natural rubber/multi walled carbon nanotubes composites. Composites Part A: Applied Science and Manufacturing.

2015;77:164-171.
17. Hoikkanen M, Poikelispää M, Das A, Honkanen M, Dierkes W, Vuorinen J. Effect of Multiwalled Carbon Nanotubes on the Properties of EPDM/NBR Dissimilar Elastomer Blends. Polymer-Plastics Technology and Engineering. 2014;54(4):402-410.
18. Perez LD, Zuluaga MA, Kyu T, Mark JE, Lopez BL. Preparation, characterization, and physical properties of multiwall carbon nanotube/elastomer composites. Polymer Engineering & Science. 2009;49(5):866-874.
19. Wu J, Chung DDL. Calorimetric study of the effect of carbon fillers on the curing of epoxy. Carbon. 2004;42(14):3039-3042.
20. Sadeghalvaad M, Dabiri E, Zahmatkesh S, Afsharimoghadam P. Preparation and properties evaluation of nitrile rubber nanocomposites reinforced with organo-clay, $CaCO_3$, and SiO2 nanofillers. Polym Bull. 2018.
21. Kueseng K, Jacob KI. Natural rubber nanocomposites with SiC nanoparticles and carbon nanotubes. Eur Polym J. 2006;42(1):220-227.
22. Dabiri E, Noori M, Zahmatkesh S. Modeling and CFD simulation of volatile organic compounds removal from wastewater by membrane gas stripping using an electro-spun nanofiber membrane. Journal of Water Process Engineering. 2018:100635.
23. Zahmatkesh S, Zebarjad SM, Bahrololoom ME, Dabiri E, Arab SM. Synthesis of ZnO/In2O3 composite nanofibers by co-electrospinning: A comprehensive parametric investigating the process. Ceram Int. 2019;45(2):2530-2541.
24. Mondal S, Nayak L, Rahaman M, Aldalbahi A, Chaki TK, Khastgir D, et al. An effective strategy to enhance mechanical, electrical, and electromagnetic shielding effectiveness of chlorinated polyethylene-carbon nanofiber nanocomposites. Composites Part B: Engineering. 2017;109:155-169.
25. Luo ZP, Koo JH. Quantitative study of the dispersion degree in carbon nanofiber/polymer and carbon nanotube/polymer nanocomposites. Mater Lett. 2008;62(20):3493-3496.
26. Tang L-C, Wan Y-J, Yan D, Pei Y-B, Zhao L, Li Y-B, et al. The effect of graphene dispersion on the mechanical properties of graphene/epoxy composites. Carbon. 2013;60:16-27.
27. El Achaby M, Arrakhiz F-E, Vaudreuil S, el Kacem Qaiss A, Bousmina M, Fassi-Fehri O. Mechanical, thermal, and rheological properties of graphene-based polypropylene nanocomposites prepared by melt mixing. Polym Compos. 2012;33(5):733-744.
28. Yazdanbakhsh A, Grasley Z, Tyson B, Abu Al-Rub RK. Dispersion quantification of inclusions in composites. Composites Part A: Applied Science and Manufacturing. 2011;42(1):75-83.
29. Glaskova T, Zarrelli M, Borisova A, Timchenko K, Aniskevich A, Giordano M. Method of quantitative analysis of filler dispersion in composite systems with spherical inclusions. Composites Sci Technol. 2011;71(13):1543-1549.
30. Tyson BM, Abu Al-Rub RK, Yazdanbakhsh A, Grasley Z. A quantitative method for analyzing the dispersion and agglomeration of nano-particles in composite materials. Composites Part B: Engineering. 2011;42(6):1395-1403.
31. Taguet A, Cassagnau P, Lopez-Cuesta JM. Structuration, selective dispersion and compatibilizing effect of (nano) fillers in polymer blends. Prog Polym Sci. 2014;39(8):1526-1563.
32. da Silva ALN, Rocha MCG, Moraes MAR, Valente CAR, Coutinho FMB. Mechanical and rheological properties of composites based on polyolefin and mineral additives. Polym Test. 2002;21(1):57-60.
33. Venkateswarlu K, Chandra Bose A, Rameshbabu N. X-ray peak broadening studies of nanocrystalline hydroxyapatite by Williamson–Hall analysis. Physica B: Condensed Matter. 2010;405(20):4256-4261.
34. 2nd International Conference on Composite Interfaces (ICCI-II) Cleveland, Ohio, USA, 13–17 June 1988. Appl Surf Sci. 1987;27(4):488.
35. Yingbin Liu, Na Li MR. Toughening poly (trimethylene terephthalate) by maleinized acrylonitrile-butadiene-styrene. Macromol An Indian J. 2013;9(3):91–101.
36. Li Y, Wu X, Song J, Li J, Shao Q, Cao N, et al. Reparation of recycled acrylonitrile- butadiene-styrene by pyromellitic dianhydride: Reparation performance evaluation and property analysis. Polymer. 2017;124:41-47.
37. Kohjiya S, Ikeda Y. Reinforcement of General-Purpose Grade Rubbers by Silica Generated In Situ. Rubber Chem Technol. 2000;73(3):534-550.
38. Kim J-t, Oh T-s, Lee D-h. Morphology and rheological properties of nanocomposites based on nitrile rubber and organophilic layered silicates. Polym Int. 2003;52(7):1203-1208.
39. Afzal M. Heuristic Model for Conical Carbon Nanofiber. University of Toledo, Toledo, OH; 2004.
40. Bussy C, Paineau E, Cambedouzou J, Brun N, Mory C, Fayard B, et al. Intracellular fate of carbon nanotubes inside murine macrophages: pH-dependent detachment of iron catalyst nanoparticles. Part Fibre Toxicol. 2013;10(1):24.
41. Salehabadi A, Salavati-Niasari M, Ghiyasiyan-Arani M. Self-assembly of hydrogen storage materials based multi-walled carbon nanotubes (MWCNTs) and $Dy_3Fe_5O_{12}$ (DFO) nanoparticles. J Alloys Compd. 2018;745:789-797.
42. Gupta VK, Agarwal S, Saleh TA. Synthesis and characterization of alumina-coated carbon nanotubes and their application for lead removal. J Hazard Mater. 2011;185(1):17-23.
43. Baldé CP, Hereijgers BPC, Bitter JH, de Jong KP. Facilitated Hydrogen Storage in NaAlH4 Supported on Carbon Nanofibers. Angew Chem. 2006;118(21):3581-3583.
44. Vellacheri R, Pillai VK, Kurungot S. Hydrous RuO_2–carbon nanofiber electrodes with high mass and electrode-specific capacitance for efficient energy storage. Nanoscale. 2012;4(3):890-896.
45. Guevara L, Welsh R, Atwater M. Parametric Effects of Mechanical Alloying on Carbon Nanofiber Catalyst Production in the Ni-Cu System. Metals. 2018;8(4):286.
46. Zou R, Li C, Zhang L, Yue D. Selective hydrogenation of nitrile butadiene rubber (NBR) with rhodium nanoparticles supported on carbon nanotubes at room temperature. Catal Commun. 2016;81:4-9.
47. Preetha Nair K, Thomas P, Joseph R. Latex stage blending of multiwalled carbon nanotube in carboxylated acrylonitrile butadiene rubber: Mechanical and electrical properties. Materials & Design. 2012;41:23-30.
48. Hanas VK and T. Development and Characterization of NBR/Silica Nanocomposites. J Mater Sci Mech Eng [Internet]. 2016;3(1):27–30.

49. Zhu J, Wei S, Ryu J, Budhathoki M, Liang G, Guo Z. In situ stabilized carbon nanofiber (CNF) reinforced epoxy nanocomposites. J Mater Chem. 2010;20(23):4937.
50. Poh BT, Ismail H, Tan KS. Effect of filler loading on tensile and tear properties of SMR L/ENR 25 and SMR L/SBR blends cured via a semi-efficient vulcanization system. Polym Test. 2002;21(7):801-806.
51. Eyssa HM, Abulyazied DE, Abdulrahman M, Youssef HA. Mechanical and physical properties of nanosilica/nitrile butadiene rubber composites cured by gamma irradiation. Egyptian Journal of Petroleum. 2018;27(3):383-392.
52. Sae-oui P, Sirisinha C, Thepsuwan U, Hatthapanit K. Dependence of mechanical and aging properties of chloroprene rubber on silica and ethylene thiourea loadings. Eur Polym J. 2007;43(1):185-193.
53. K.Rajkumar, Prem Ranjan, P.Thavamani, P.Jeyanthi PP. DISPERSION STUDIES OF NANOSILICA IN NBR BASED POLYMER NANOCOMPOSITE. Rasayan J Chem. 2013;6(2):122–33.
54. Al-Hosney HA, Grassian VH. Water, sulfur dioxide and nitric acid adsorption on calcium carbonate: A transmission and ATR-FTIR study. PCCP. 2005;7(6):1266.